Self-Assembly of a Two-Dimensional Coordination Polymer Based on Silver and Lanthanide Tetrakis-Acylpyrazolonates: An Efficient New Strategy for Suppressing Ligand-to-Metal Charge Transfer Quenching of Europium Luminescence

Yury A. Belousov [1,2,*] , **Mikhail T. Metlin** [2] , **Darya A. Metlina** [2] , **Mikhail A. Kiskin** [3] , **Ilya A. Yakushev** [3] , **Trofim A. Polikovskiy** [2] , **Ilya V. Taydakov** [2] , **Andrei A. Drozdov** [1] , **Fabio Marchetti** [4] and **Claudio Pettinari** [5]

[1] Chemistry Department, M.V. Lomonosov Moscow State University, Leninskie Gory Str, Building 1/3, 119991 Moscow, Russia

[2] P. N. Lebedev Physical Institute of Russian Academy of Sciences, Leninsky Prospect 53, 119991 Moscow, Russia

[3] Kurnakov Institute of General and Inorganic Chemistry of the Russian Academy of Sciences, Leninsky Prospekt 31, 119991 Moscow, Russia

[4] School of Science and Tecnology, Chemistry Interdisciplinary Project (ChIP), University of Camerino, Via Madonna delle Carceri, 62032 Camerino, Italy

[5] School of Pharmacy, Chemistry Interdisciplinary Project (ChIP), University of Camerino, Via Madonna delle Carceri, 62032 Camerino, Italy

* Correspondence: belousov@inorg.chem.msu.ru

Abstract: A new strategy for the easy polymerization of anionic $[Ln(Q^{cy})_4]^-$ (HQ^{cy}-4-(cyclohexanecarbonyl)-5-methyl-2-phenyl-2,4-dihydro-3H-pyrazol-3-one) into two-dimensional layers of $[AgLn(Q^{cy})_4]_n$ (Ln = Sm, Eu, Gd, Tb and Dy) is proposed by binding the single molecular anions $[Ln(Q^{cy})_4]^-$ to silver cations through the coordination of the pyridinic nitrogen atoms of the pyrazolonate rings. The luminescent properties of $[AgLn(Q^{cy})_4]_n$ have been studied in detail, and it was shown that the previously described low photoluminescence quantum yield (PLQY) of $[Eu(Q^{cy})_4]^-$ is due to Ligand-To-Metal Charge Transfer (LMCT) quenching, which is effectively suppressed in the heterometallic $[AgEu(Q^{cy})_4]_n$ polymer. Sensibilization coefficients for $H_3O[Eu(Q^{cy})_4]$, $[AgEu(Q^{cy})_4]_n$, and $H_3O[Sm(Q^{cy})_4]$ complexes (n ≈ 1) were estimated via theoretical analysis (also by using Judd-Ofelt theory for Sm^{3+}) and PLQY measurements.

Keywords: lanthanides; luminescence; LMCT quenching; silver; pyrazolonates; europium; heterometallic complexes; coordination polymers

1. Introduction

Coordination polymers (CPs) of various dimensions, including porous MOF materials, are attracting unrelenting interest from materials scientists and chemists due to the combination of unique functional properties (magnetic, catalytic, or luminescent) of individual molecular units with the stability of polymeric materials and the presence of pores and channels capable of reversible sorption of guest molecules [1,2]. Undoubtedly, the respectable place in the chemistry of coordination polymers is occupied by lanthanides derivatives [3–5]. The directed synthesis of CPs based on the Ln^{3+} ions is complicated by high and variable values of coordination numbers, as well as the absence of preferred polyhedra for *4f*-elements [6,7]. At the same time, the luminescent properties of lanthanide complexes, due to the unique features of the electronic configuration, find application in the creation of various materials for light-emitting devices (LEDs) [8–11], biological luminescent labels [12–14], in thermometry [15–17] and in chemical sensors [18–23].

The most common approach to solve all these problems involves the use of antenna sensitization of lanthanide luminescence, i.e., inclusion in the complex of organic ligands

capable of effectively absorbing exciting radiation and transmitting it to the emission center, the lanthanide cation [6,24–26]. Among the anionic ligands, the most effective luminescence sensitizers, β-diketones stand out, which, nevertheless, usually form mononuclear complexes [Ln(β-diketone)$_3$(L)$_{1-2}$] or molecular anions [Ln(β-diketone)$_4$]$^-$, which are soluble in typical organic solvents and have moderate chemical stability [27]. The monomeric nature of most studied Ln^{3+} diketonates can complicate functional applications in a number of problems, for example, in the creation of sensor materials [22,23]. To create oligomeric and polymeric lanthanide coordination compounds, it is necessary to use polydentate ligands, such as carbocyclic [28] and heterocyclic [5] aromatic carboxylic acids, which often have absorption maxima with λ < 300 nm and have low absorption in the near UV region (300–400 nm). Less than 10% of the approximately 4000 structures of lanthanide diketonates deposited in the Cambridge Crystal Data Centre (CCDC) have a polymeric structure. However, some methods are now known for linking diketonate complexes into coordination polymers. This goal can be achieved by introducing additional donor atoms into the ligand structure (as, for example, in pyrazole- [29], imidazole- [30], or pyridine-containing [31–35] β-diketones), or by using additional linker ligands, such as bis(diphenylphosphine oxides) [36–42], 4,4'-bipyridyl [43] or its N-oxide [44], quinone-based ligands [45], 2,2'-bipyrimidine [46] etc. Tetrakis anions [Ln(β-diketone)$_4$]$^-$ can be polymerized by forming alkali metal salts under non-aqueous conditions [47–49]. In most of the mentioned cases, the dimensionality of the polymer is limited by the coordination number of the lanthanide: if in a typical complex with CN = 8 three diketonate ligands occupy six positions, then the polymer is forced to be linear.

In the chemistry of lanthanides, among β-diketone-related ligands, a special role is played by acylpyrazolones [50–52] containing a heterocyclic pyrazolone fragment as a component of the β-diketonate system. This is due to the high energies of the triplet level in comparison with common aromatic β-diketones, such as dibenzolylmethane and thenoyltrifluoroacetone, which make it possible to effectively sensitize the luminescence of Tb^{3+} [53–56] and Dy^{3+} [57–59] ions. Acylpyrazolonates of these metals have been repeatedly tested as emitting layers in OLED devices [53,54,56,58] showing high efficiency values. In all cases, the coordination of lanthanides occurs at the acylpyrazolonate Q$^-$ site with the formation of neutral tris complexes [LnQ$_3$(L)$_{1-2}$] [37,57,60–66] or tetrakis anions [LnQ$_4$]$^-$ [57,67–69], or dimers [LnQ$_3$]$_2$ [70–72].

Previously, coordination polymers based on rare-earth acylpyrazolonates were obtained only through the use of bridged ligands of the phosphine oxide series [36,37]. In the present paper, we report a fundamentally new approach to the creation of coordination polymers due to the binding of [Ln(Q^{cy})$_4$]$^-$ anions by Ag$^+$ cations through nitrogen atoms of pyrazole rings with the formation of 2D-MOF [AgLn(Q^{cy})$_4$]$_n$, where Ln = Sm-Dy, and HQ^{cy} = 4-(cyclohexanecarbonyl)-5-methyl-2-phenyl-2,4-dihydro-3H-pyrazol-3-one. Such a reaction is possible due to the fact that silver cations, being soft Pearson acids, form complexes with diketonate ligands [73] only with difficulty, preferring coordination with softer donor atoms, for example, the nitrogen atom [73,74]. Moreover, the H$_3$O[Ln(Q^{cy})$_4$] (Ln = Sm, Tb, Dy) coordination compounds have pronounced ion-centered luminescence with the quantum yields (~2, 56 and 3%, respectively) close to the highest ones to date [75,76]. However, a curiously low value of overall PLQY was obtained for the H$_3$O[Eu(Q^{cy})$_4$] complex, below the measurement limit. From our investigation we could state that this uncommon result is due to the luminescence quenching via LMCT. Effective suppression of the LMCT processes was accomplished by the new method, provided in our research, of a change-over to polymer complexes with an Ag$^+$ ion instead of H$_3$O$^+$ in the outer coordination sphere. Specifically, we were able to totally prevent the LMCT participation in the luminescent process in the [AgEu(Q^{cy})$_4$]$_n$ complex with significantly high PLQY increase of up to two orders compared to the H$_3$O[Eu(Q^{cy})$_4$] one.

2. Materials and Methods

2.1. Synthesis and Spectroscopic Characterization of the Complexes

The hydroxonium complexes $H_3O[Ln(Q^{cy})_4]$ were prepared according to the procedure previously reported [57] for a $H_3O[Dy(Q^{cy})_4]$ complex using $LnCl_3$ hexahydrates as starting reagents. The isostructurality of the complexes **1–5** was confirmed by powder diffraction (see SI, Figure S1).

$H_3O[Sm(Q^{cy})_4]$, 1. Pale yellow plates, 78%. Anal. Calc. for $C_{68}H_{79}N_8O_9Sm$: C, 62.69; H, 6.11; N, 8.60; Sm, 11.54%. Found: C, 62.0; H, 6.7; N, 8.5; Sm, 11.9. IR (cm^{-1}): 3392 m (ν O–H^{H3O+}), 2929 m, 2853 m (ν C-H^{Cyclohexyl}), 1662 w (δ O–H^{H3O+}), 1612 m (ν C=O^{Diketone}), 1593 m, 1584 m, 1499 m (ν C–C), 1400 m, 1235 m, 1145 w, 1078 vs, 1027 s, 902 m, 812 m, 691 w.

$H_3O[Eu(Q^{cy})_4]$, 2. Colorless plates, 73%. Anal. Calc. for $C_{68}H_{79}N_8O_9Eu$: C, 62.62; H, 6.10; N, 8.59; Eu, 11.65%. Found: C, 62.5; H, 6.7; N, 8.6; Eu, 12.0. IR (cm^{-1}): 3392 m (ν O–H^{H3O+}), 2929 m, 2852 m (ν C-H^{Cyclohexyl}), 1662 w (δ O–H^{H3O+}), 1614 m (ν C=O^{Diketone}), 1593 m, 1584 m, 1499 m (ν C–C), 1400 m, 1232 m, 1145 w, 1078 vs, 1028 s, 902 m, 812 m, 692 w.

$H_3O[Gd(Q^{cy})_4]$, 3. Colorless plates, 74%. Anal. Calc. for $C_{68}H_{79}N_8O_9Gd$: C, 62.36; H, 6.08; N, 8.56; Gd, 12.01%. Found: C, 62.1; H, 6.4; N, 8.4; Gd, 12.2. IR (cm^{-1}): 3391 m (ν O–H^{H3O+}), 2930 m, 2852 m (ν C-H^{Cyclohexyl}), 1661 w (δ O–H^{H3O+}), 1616 m (ν C=O^{Diketone}), 1592 m, 1584 m, 1500 m (ν C–C), 1400 m, 1232 m, 1145 w, 1078 vs, 1028 s, 902 m, 812 m, 692 w.

$H_3O[Tb(Q^{cy})_4]$, 4. Colorless plates, 73%. Anal. Calc. for: $C_{68}H_{79}N_8O_9Tb$: C, 62.28; H, 6.07; N, 8.55; Tb, 12.12%. Found: C, 62.5; H, 6.2; N, 8.6; Tb, 11.7. IR (cm^{-1}): 3391 m (ν O–H^{H3O+}), 2929 m, 2852 m (ν C-H^{Cyclohexyl}), 1661 w (δ O–H^{H3O+}), 1616 m (ν C=O^{Diketone}), 1593 m, 1584 m, 1500 m (ν C–C), 1400 m, 1230 m, 1145 w, 1078 vs, 1028 s, 902 m, 812 m, 692 w.

$H_3O[Dy(Q^{cy})_4]$, 5. Pale yellow plates, 70%. Anal. Calc. for $C_{68}H_{79}N_8O_9Dy$: C, 62.11; H, 6.06; N, 8.52; Dy, 12.36%. Found: C, 61.9; H, 6.1; N, 7.9%. IR (cm^{-1}): 3390 m (ν O–H^{H3O+}), 2929 m, 2852 m (ν C-H^{Cyclohexyl}), 1660 w (δ O–H^{H3O+}), 1616 m (ν C=O^{Diketone}), 1594 m, 1584 m, 1500 m (ν C–C), 1400 m, 1230 m, 1153 w, 1078 vs, 1028 s, 902 m, 812 m, 692w.

The silver complexes $[AgLn(Q^{cy})_4]_n$ **6–10** were obtained according to the following general procedure given in detail for $[AgSm(Q^{cy})_4]_n$.

$[AgSm(Q^{cy})_4]_n$, 6. 0.069 mg (0.222 mmol) of a $SmCl_3·6H_2O$ and 1.5 mL of H_2O were placed in a centrifugation tube. Then, 0.100 mL of a NH_3 solution ~12 M were added, the volume was adjusted to 2 mL with water and centrifuged (8000 rpm, 5 min). The precipitate was carefully washed with water (4 × 2 mL), 96% ethanol (2 × 2 mL) and added to a solution of 0.284 g (1.00 mmol) of HQ^{cy} in 20 mL of 96% ethanol at room temperature. The mixture was stirred without heating until the precipitation of the formed lanthanide hydroxide. Then, 0.224 mL of a 10% solution of triethylamine (0.222 mmol) in 96% ethanol was added dropwise and the solution was filtered through a 0.25 μm PTFE syringe membrane filter. Subsequent operations were performed in the dark.

A solution of 0.0377 g (0.222 mmol) silver nitrate in 5 mL of acetonitrile was added dropwise at a rate of 1 mL per minute. An abundant precipitate begins to form already when the first drops are added. The suspension was stirred at room temperature for another 15 min, after which it was filtered on a glass porous filter, washed with ethanol (2 × 5 mL), acetonitrile (2 × 5 mL) and diethyl ether (2 × 5 mL). The precipitate was dried in a darkened desiccator over P_4O_{10} for 48 h.

$[AgSm(Q^{cy})_4]_n$, 6. Pale yellow powder, 82%. Anal. Calc. for $C_{68}H_{76}N_8O_8AgSm$: C, 58.69; H, 5.50; N, 8.05; Ag, 7.75; Sm, 10.80%. Found: C, 58.2; H, 5.6; N, 8.0; Ag, 7.5; Sm, 11.3%. IR (cm^{-1}): 3058 m, 2929 m, 2852 m(ν C-H^{Cyclohexyl}), 1627 vs (ν C=O^{Diketone}), 1600 m, 1500 s, 1434 w, 1395 w, 1370 w, 1080 m, 1035 vw, 1010 vw, 979 m, 812 vw, 758 w, 693 w, 622 w, 452 w.

$[AgEu(Q^{cy})_4]_n$, 7. White powder, 83%. Anal. Calc. for $C_{68}H_{76}N_8O_8AgEu$: C, 58.62; H, 5.50; N, 8.04; Ag, 7.74; Eu, 10.91%. Found: C, 58.9; H, 5.5; N, 8.2; Ag, 7.6; Eu, 10.8%.

IR (cm^{-1}): 3060 m, 2929 m, 2852 m(ν C-H^{Cyclohexyl}), 1628 vs (ν C=O^{Diketone}), 1599 m, 1500 s, 1435 w, 1392 w, 1377 vw, 1080 m, 1010 w, 979 m, 756 w, 691 w, 623 w, 450 w.

[AgGd(Q^{cy})$_4$]$_n$, 8. White powder, 74%. Anal. Calc. for C$_{68}$H$_{76}$N$_8$O$_8$AgGd: C, 58.40; H, 5.48; N, 8.01; Ag, 7.71; Gd, 11.24%. Found: C, 58.2; H, 5.8; N, 8.0; Ag, 7.7; Gd, 11.4%. IR (cm^{-1}): 3061 m, 2929 m, 2852 m (ν C-H^{Cyclohexyl}), 1628 vs(ν C=O^{Diketone}), 1598 m, 1500 s, 1436 w, 1392 w, 1372 vw, 1080 m, 1010 w, 978 m, 756 w, 690 w, 623 w, 448 vw.

[AgTb(Q^{cy})$_4$]$_n$, 9. White powder, 82%. Anal. Calc. for C$_{68}$H$_{76}$N$_8$O$_8$AgTb: C, 58.33; H, 5.47; N, 8.00; Ag, 7.70; Tb, 11.35%. Found: C, 58.4; H, 5.6; N, 8.2; Ag, 7.7; Tb, 11.4%. IR (cm^{-1}): 3070 m, 2928 m, 2852 m, (ν C-H^{Cyclohexyl}) 1631 vs(ν C=O^{Diketone}), 1596 m, 1501 s, 1543, 1435 w, 1371 w, 1080 m, 979 m, 902 vw, 756 w, 691 w, 622 w, 449 w.

[AgDy(Q^{cy})$_4$]$_n$, 10. White powder, 77%. Anal. Calc. for C$_{68}$H$_{76}$N$_8$O$_8$AgDy: C, 58.18; H, 5.46; N, 7.98; Ag, 7.68; Dy, 11.58%. Found: C, 58.6; H, 5.2; N, 7.9; Ag, 7.8; Dy, 11.2%. IR (cm^{-1}): 3071 m, 2929 m, 2852 m (ν C-H^{Cyclohexyl}), 1631 vs(ν C=O^{Diketone}), 1595 m, 1502 s, 1542, 1435 w, 1371 w, 1081 m, 979 m, 692 w, 622 w, 449 w.

Single crystals of [AgGd(Q^{cy})$_4$]$_n$ (**8**) were obtained by suspending 0.05 g of the powder in 10 mL of acetonitrile at room temperature in the dark. The precipitate was then separated by centrifugation (8000 rpm), and the solution was filtered through a 0.25 μm PTFE syringe membrane filter. Slow evaporation of the solution at room temperature allowed the obtaining of small single crystals of **8** suitable for investigations on the synchrotron equipment. The isostructurality of other compounds **6**, **7**, **9** and **10** was confirmed by powder diffraction methods (see SI, Figure S2).

2.2. Apparatus

Elemental analyses were performed with an Elemental Vario MicroCube CHNO(S) (Elementar Americas Inc., Ronkonkoma, NY, USA) analyser. The Ln^{3+} content was determined by complexometric titration with a Trilon B solution in the presence of Xylenol Orange as an indicator [77]. The silver content was determined by titration with standard KSCN solution using Fe^{3+} to indicate the end point [78]. Before the analysis, the complexes were decomposed by heating with concentrated HNO$_3$.

Absorption spectra for all the complexes were obtained on a JASCO V-770 (Jasco, Tokyo, Japan) spectrophotometer operating within 200–3200 nm. Concentrations of the solutions were approximately 10^{-5} M. For solutions, the measurements were performed using quartz cells with a 1 cm pathlength.

IR spectra were registered in the range 4000–400 cm^{-1} in KBr pellets using a Perkin-Elmer system Spectrum One 100 FTIR spectrometer (PerkinElmer, Inc., Waltham, MA, USA).

The X-ray diffraction data sets for crystals of H$_3$O[Ln(Q^{cy})$_4$] (**1**: Ln = Sm; **2**: Ln = Eu; **3**: Ln = Gd; **4**: Ln = Tb) were collected on a Bruker SMART APEX II (Bruker, Billerica, MA, USA) diffractometer equipped with a CCD detector (Mo-K$_\alpha$, λ = 0.71073 Å, graphite monochromator) [79]. X-ray diffraction data for [AgGd(Q^{cy})$_4$]$_n$ **8** were collected on the 'Belok' beamline of the Kurchatov Synchrotron Radiation Source (National Research Center 'Kurchatov Institute', Moscow, Russia) in φ-scan mode with 1° step (λ = 0.79312 Å) using a Rayonix SX165 (Rayonix, L.L.C., Evanston, IL, USA) CCD detector [80]. The structures were solved by direct methods and refined by the full-matrix least squares in the anisotropic approximation for non-hydrogen atoms. The calculations were carried out by the SHELX-2014/2018 program package [81] using Olex2 1.2 [82]. The hydrogen atoms of the ligands were positioned geometrically and refined using the riding model. Solvent molecules in [AgGd(Q^{cy})$_4$]$_n$ **8** which could not be localized were removed by the SQUEEZE procedure [83]. The crystallographic parameters for investigated crystals and the structure refinement details are given in Table 1. Crystallographic data for structures reported in this paper have been deposited with the Cambridge Crystallographic Data Center (H$_3$O[Eu(Q^{cy})$_4$]— 2233167, H$_3$O[Gd(Q^{cy})$_4$]—2233168, H$_3$O[Tb(Q^{cy})$_4$]—2233169, [AgGd(Q^{cy})$_4$]$_n$—2233170).

Photoluminescence and excitation spectra in the visible region for all the complexes were measured in solid state using a Horiba Jobin-Yvon Fluorolog QM-75-22-C spectrofluorimeter with an installed 75 W xenon arc lamp (PowerArc, HORIBA, Ltd., Kyoto, Japan).

A Hamamatsu R13456 cooled photomultiplier tube sensitive in the UV-Vis-NIR region (200–950 nm) was used as the detector. For the NIR spectral region measurements the same setup was used, except for the detector, which was replaced by a Hamamatsu H10330 (Hamamatsu Photonics, Hamamatsu, Japan) cooled photomultiplier tube sensitive in the NIR region (950–1700 nm). Photoluminescent decays in the visible region were recorded for all the complexes in solid state on the same device; however, the excitation source was changed to a pulsed xenon lamp with a 50 μs pulse duration and 100 Hz repetition rate.

Table 1. The main crystallography data and refinement details for structures $H_3O[Ln(Q^{cy})_4]$ (**1–4**) and $[AgGd(Q^{cy})_4]_n$ **8**.

Complex/Parameters	1 [a]	2	3	4	8
Empirical formula		$C_{68}H_{79}EuN_8O_9$	$C_{68}H_{79}GdN_8O_9$	$C_{68}H_{79}N_8O_9Tb$	$C_{68}H_{76}AgGdN_8O_8$
Formula weight		1304.35	1309.64	1311.31	1398.48
Crystal system			Monoclinic		
Space group	C		$C2/c$		$P2_1/n$
T, K	296	296	150	150	100
a, Å	14.907 (8)	14.8703 (6)	14.8096 (5)	14.7960 (5)	15.0083 (11)
b, Å	25.244 (16)	25.2111 (14)	25.1474 (9)	25.1641 (11)	17.7224 (16)
c, Å	16.773 (10)	16.9977 (11)	16.7390 (9)	16.7208 (9)	25.1710 (19)
β, deg.	93.87 (2)	94.7700 (10)	94.1050 (10)	94.3260 (10)	92.623 (3)
V, Å^3	6297 (2)	6350.3 (6)	6218.0 (5)	6207.9 (5)	6688.0 (9)
Z		4	4	4	4
D_{calc}, g cm^3		1.364	1.399	1.403	1.389
μ, mm^{-1}		1.051	1.131	1.204	1.782
θ_{max}, deg.		27.10	30.52	26.61	29.716
Index ranges		$-18 \leq h \leq 19$ $-32 \leq k \leq 32$ $-19 \leq l \leq 21$	$-20 \leq h \leq 21$ $-35 \leq k \leq 35$ $-23 \leq l \leq 23$	$-18 \leq h \leq 18$ $-31 \leq k \leq 31$ $-19 \leq l \leq 21$	$-18 \leq h \leq 18$ $-22 \leq k \leq 22$ $-31 \leq l \leq 31$
F (000)		2712	2716	2720	2860
R_{int}		0.1612	0.1319	0.0697	0.2473
Number of collected/total reflections		34,077/7002	37,516/9476	28,718/6414	60,971/13,654
Number of reflections ($I > 2\sigma(I)$)		5265	6920	5570	4961
Number of parameters		393	395	395	779
GooF		1.060	1.077	1.095	0.881
R_1, wR_2 ($I > 2\sigma(I)$)		0.0699, 0.1542	0.0875, 0.1535	0.0467, 0.0980	0.0911/0.1939
$\Delta\rho_{max}$, ρ_{min}(e/Å^3)		0.895, -1.774	5.325, -2.815	1.467, -1.238	0.783/-2.114

[a] Only cell parameters were determined.

Photoluminescence quantum yields were obtained for solid samples by the absolute method with the use of the same experimental setup, equipped by integration sphere G8 (GMP, Renens, Switzerland).

For all optical measurements, the corresponding instrument response functions were taken into account. The experiments were performed in air at atmospheric pressure. Degradation of the optical properties was not observed during the experiments. Commercially available reagents and solvents (Sigma-Aldrich, Darmstadt, Germany) were used as received. Ln^{3+} chlorides were obtained by dissolution of the corresponding oxides (99.999%, LANHIT, Moscow, Russia) in concentrated hydrochloric acid (reagent grade, XPC). Ligand HQ^{cy} was prepared according to the published method [37].

3. Results

3.1. Synthesis

The synthesis of complex tetrakis acids $H_3O[Ln(Q^{cy})_4]$ was carried out according to the general procedure proposed by us for a dysprosium derivative [57]. Temperature control is important to avoid formation of tris complexes $[Ln(Q^{cy})_3(H_2O)]$ [57,84]. Polymer complexes

can be obtained by the reaction of silver (I) nitrate with a solution of $H_3O[Ln(Q^{cy})_4]$ acids, but the yield of the reaction somewhat increases after its preliminary neutralization with the use of triethylamine. The complexes gradually darken in the light, so all operations must be performed in subdued light. The polymer structure makes $[AgLn(Q^{cy})_4]_n$ complexes extremely poorly soluble in most common solvents. The use of DMF for recrystallization is impossible, since it is accompanied by the decomposition of the complex with the formation of a silver mirror on the walls of the vessel. DMSO also causes decomposition of the complexes with the formation of an unspecified black precipitate (possibly silver sulfide). Among other tested solvents (methanol, ethanol, acetone, chloroform, ethyl acetate), only acetonitrile can be a possible medium for recrystallization. Attempts to grow large crystals under solvothermal conditions were unsuccessful, and only small crystals of the gadolinium complex were studied at the synchrotron facility. However, IR spectroscopy, elemental analysis, and powder diffraction data confirm that all $[AgLn(Q^{cy})_4]_n$ complexes are isomorphic to the gadolinium polymeric complex $[AgGd(Q^{cy})_4]_n$.

3.2. Single Crystal Structures

Complexes $[H_3O][Ln(Q^{cy})_4]$ **1–4** (**1**: Ln = Sm; **2**: Ln = Eu; **3**: Ln = Gd; **4**: Ln = Tb) crystallize in the monoclinic space group C2/c (for crystals with Ln = Sm, only cell parameters were determined; Table 1) and are isostructural to the previously described dysprosium complex $[H_3O][Dy(Q^{cy})_4]$ **5** [57]. These compounds consist of the $[Ln(Q^{cy})_4]^-$ anion and of the outer sphere H_3O^+ (Figure 1a). The Ln atom is coordinated by four chelating Q^{cy} ligands to form a LnO_8 polyhedron in a square antiprismatic geometry (main distances and angles are given in Table 2). The oxygen atom of H_3O^+ is disordered in two positions (a two-fold axis passes between them) and form H-bonds with two N atoms of one complex molecule and one N atom of the neighboring molecule (Figure 2a; Table S1). Additionally, the molecule is stabilized by intramolecular C-H ... O/N as well as C-H ... π interactions (Tables S1 and S2). In the crystal, π-π intermolecular interactions occur between the pyrazole rings of neighboring molecules (Table S3). As in the other described $H(H_2O)_n[LnQ_4]$ tetrakis-acids, stabilization is achieved by strong intermolecular hydrogen bonds [57,67–69]. H-bonding between the anionic fragments $[Ln(Q^{cy})_4]^-$ leads to the formation of 1D supramolecular chains.

(**a**)   (**b**)
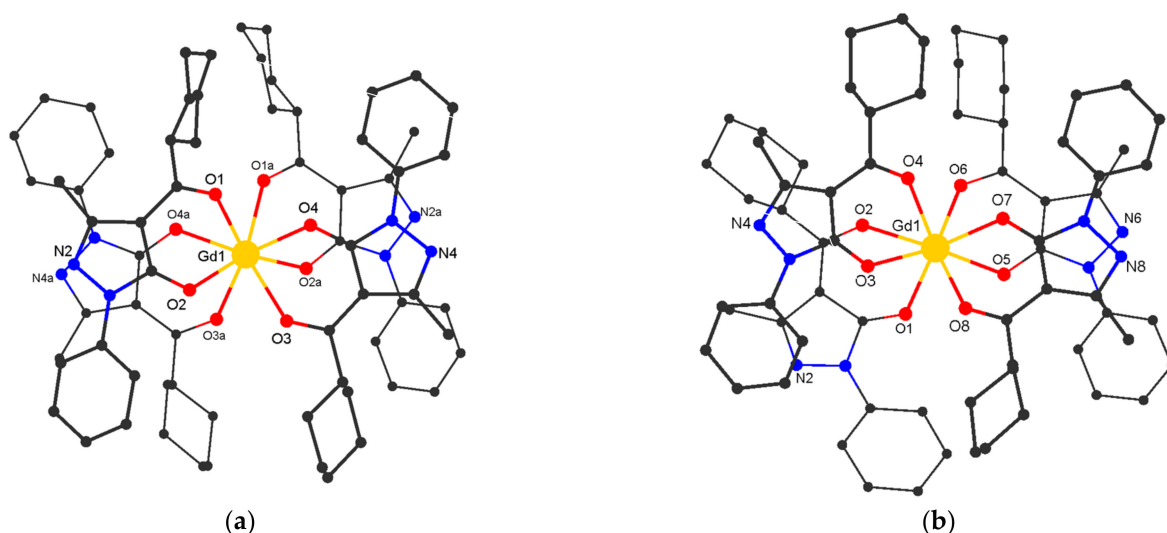
Figure 1. Structure of the anionic moiety of **[Gd(Q^{cy})$_4$]$^-$** in **H$_3$O[Gd(Q^{cy})$_4$] 3** (**a**) and in **[AgGd(Q^{cy})$_4$]$_n$ 8** (**b**) (H atoms are omitted).

Table 2. Selected bond lengths, shortest interatomic distances (Å), angles (deg.) and symmetry of polyhedron LnO_8 in $H_3O[Ln(Q^{cy})_4]$ **2–4** (Ln = Eu, Gd, Tb) and $[AgGd(Q^{cy})_4]_n$ **8**.

Complex/Parameter	2	3	4	8
Ln-O	2.354 (4)–2.436 (4)	2.349 (4)–2.414 (4)	2.328 (3)–2.412 (3)	2.287 (8)–2.448 (9)
O-Ln-O (1,3-diketone)	71.14 (13), 72.13 (14)	71.75 (13), 72.28 (14)	72.22 (9), 72.66 (9)	68.1 (3)–70.8 (3)
Ag-N	-	-	-	2.229 (11)–2.403 (9)
N-Ag-N	-	-	-	99.4 (4), 129.3 (4), 131.2 (4)
Symmetry of the LnO_8 polyhedron with S_Q (p) value [a]	Square antiprism, D_{4d}, 0.322	Square antiprism, D_{4d}, 0.254	Square antiprism, D_{4d}, 0.246	Square antiprism, D_{4d}, 0.322

[a] The geometry of the polyhedron corresponds to the symmetry of the analyzed environment; the details of the analysis of the polyhedron are given in Table S4.

(**a**)

(**b**)
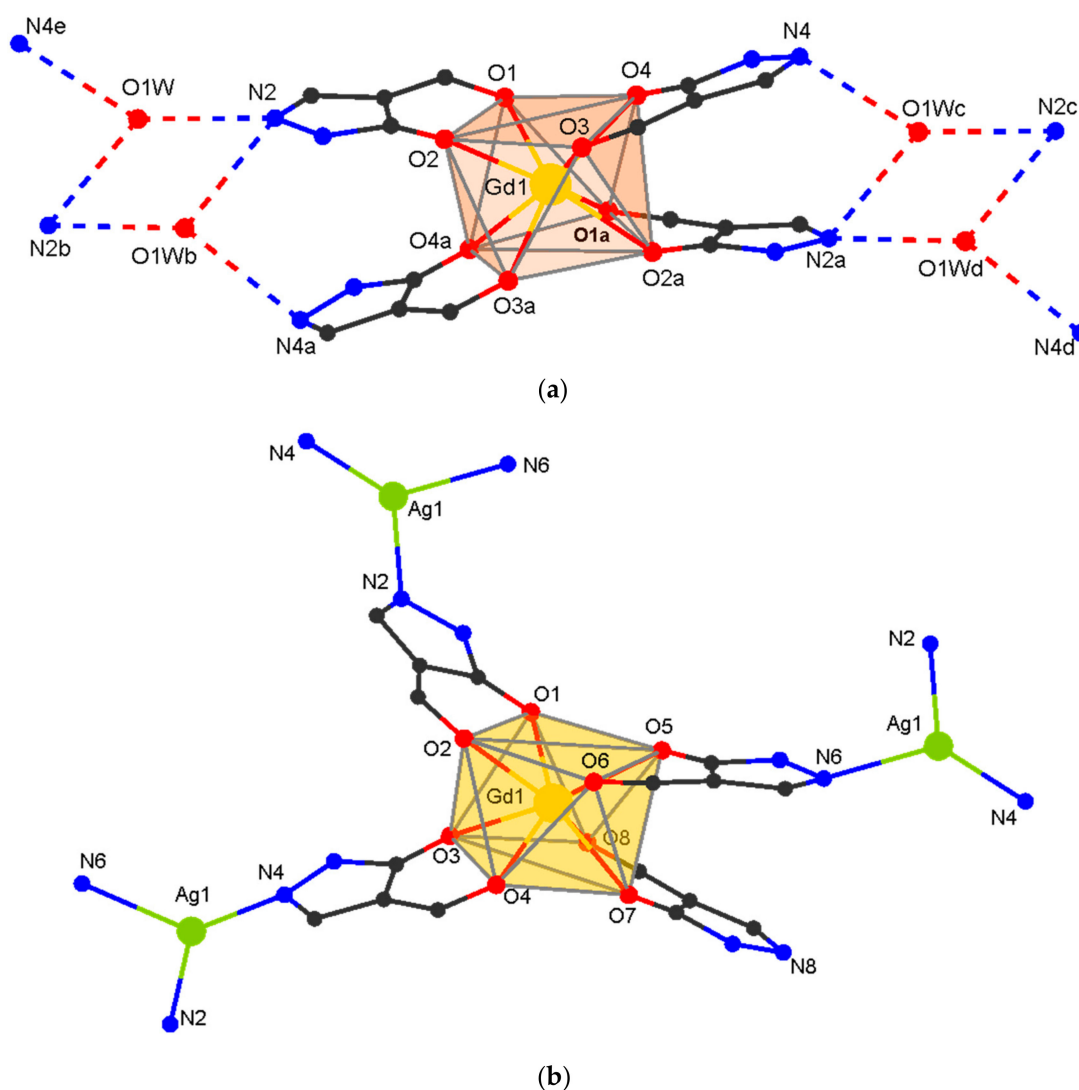
Figure 2. Fragment of the crystal packing in $H_3O[Gd(Q^{cy})_4]$ **3** (**a**) and $[AgGd(Q^{cy})_4]_n$ **8** (**b**) (phenyl, cyclohexyl and methyl groups are omitted for clarity).

$[AgGd(Q^{cy})_4]_n$ **8** crystallizes in the monoclinic space group P2$_1$/n. It contains the fragment $[Gd(Q^{cy})_4]$ and the Ag center. The structure of the $[Gd(Q^{cy})_4]^-$ fragment in **8** is similar to that in **3** (Figure 1b), the geometry of the metal atoms environment (GdO$_8$) being slightly distorted (Figure 2, Table 2). The molecule is stabilized by intramolecular C-H . . . O/N interactions (Table S1). Each Ag atom is coordinated by three pyridinic N atoms of the pyrazole rings from three $[Gd(Q^{cy})_4]$ fragments. Each $[Gd(Q^{cy})_4]$ fragment is bonded

to three Ag atoms; thus, three of the four pyrazole rings are involved in formation of the polymeric structure (Figure 2b). Binding of $[Gd(Q^{cy})_4]^-$ to Ag^+ leads to the formation of a layered structure with a well-known topological type **fes** [85], where both structural building units are 3-coordinated nodes (Figure 3). In the crystal, π-π intermolecular interactions occur between the pyrazole and the phenyl rings of neighboring anionic framents (Table S3). The minimum interatomic distance between successive Gd atoms in the layer is 8.788 Å, and that of neighboring layers is 13.040 Å. The interlayer space is filled by cyclohexyl substituents.
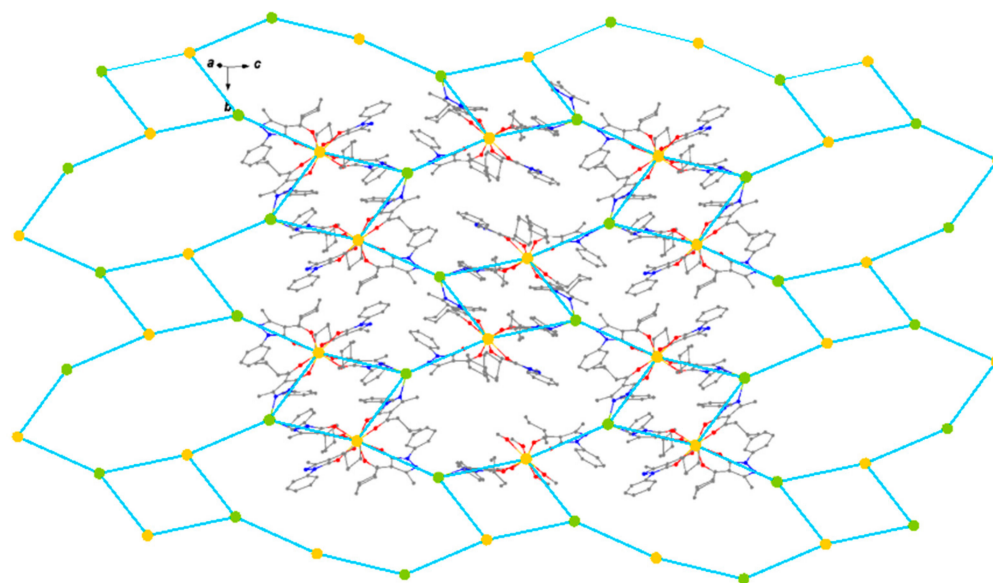

Figure 3. Crystal packing of $[AgGd(Q^{cy})_4]_n$ **8**.

3.3. Optical Properties

The absorption spectra of $H_3O[Ln(Q^{cy})_4]$ **1–4** dissolved in MeCN are shown in Figure 4. All complexes **1–4** reveal intensive absorption in the range 250–375 nm. The observed absorption maximum at 265 nm is originated from the π-π^* transition in the β-diketone moiety [57]. The spectra qualitatively resemble each other; therefore, despite the variation of the central ion, the ligand environment energy structure remains the same. Moreover, the coordination of the central ion by the ligands allows an increase in the molar extinction of the complexes up to 10^5 L $\times$ mol^{-1} $\times$ cm^{-1}, with respect to the low values obtained for the free ions (~10 L $\times$ mol^{-1} $\times$ cm^{-1}). Notably, we did not observe any absorption bands related to ion transitions due to a high ligand absorption rate.

The energy of the first excited singlet state (S_1) was estimated using the tangent method [26] for the absorption spectra. For all the complexes, the S_1 energies are nearly equal and are 27,300 cm^{-1}. Due to the low solubility of $[AgLn(Q^{cy})_4]_n$ **6–10** in most of the solvents generally employed (acetonitrile, methanol, dichloromethane), it is impossible to record their absorption spectra. For this reason, diffuse reflectance spectra were studied (see below).

PL excitation spectra, recorded for all the complexes in the solid state, are shown in Figure 5. Apart from $H_3O[Eu(Q^{cy})_4]$, all the other complexes reveal the strong ion-centered luminescence under the optical excitation in a wide spectral range from 285 to 425 nm. The wide excitation band with the maximum at 340 nm is specific of the sensitization of the luminescence through the π^*-π transition in the β-diketone moiety. However, the spectrum of the $H_3O[Eu(Q^{cy})_4]$ shows a maximum at 380 nm with the FWHM (full width at half maximum) of 75 nm. We suggest that this band is related to the excitation due to ligand-to-metal charge-transfer (LMCT) [86]. Actually, the long wavelength shoulder observed for **2** in the diffuse reflection spectrum (see Figure 6) can result from different charge transfer processes. No LMCT with such energies has been observed for **4** due to

the high redox potential of terbium ion. As the spectrum of **4** reveals no absorption within 360–450 nm, the shoulder in **2** can be associated to LMCT.
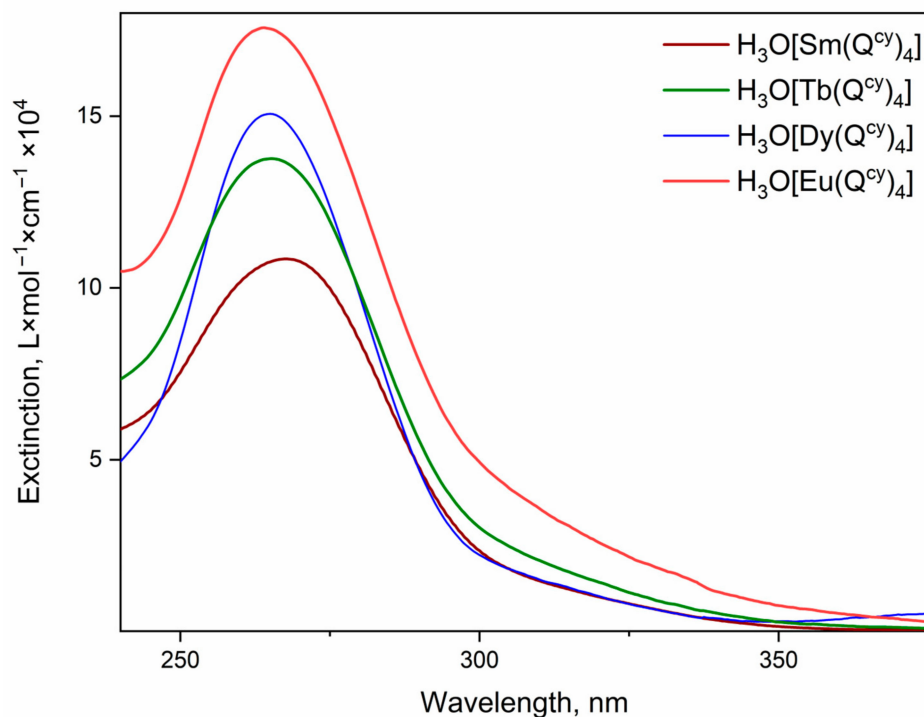

Figure 4. UV-VIS spectra of [H$_3$O][Ln(Q^{cy})$_4$] complexes.
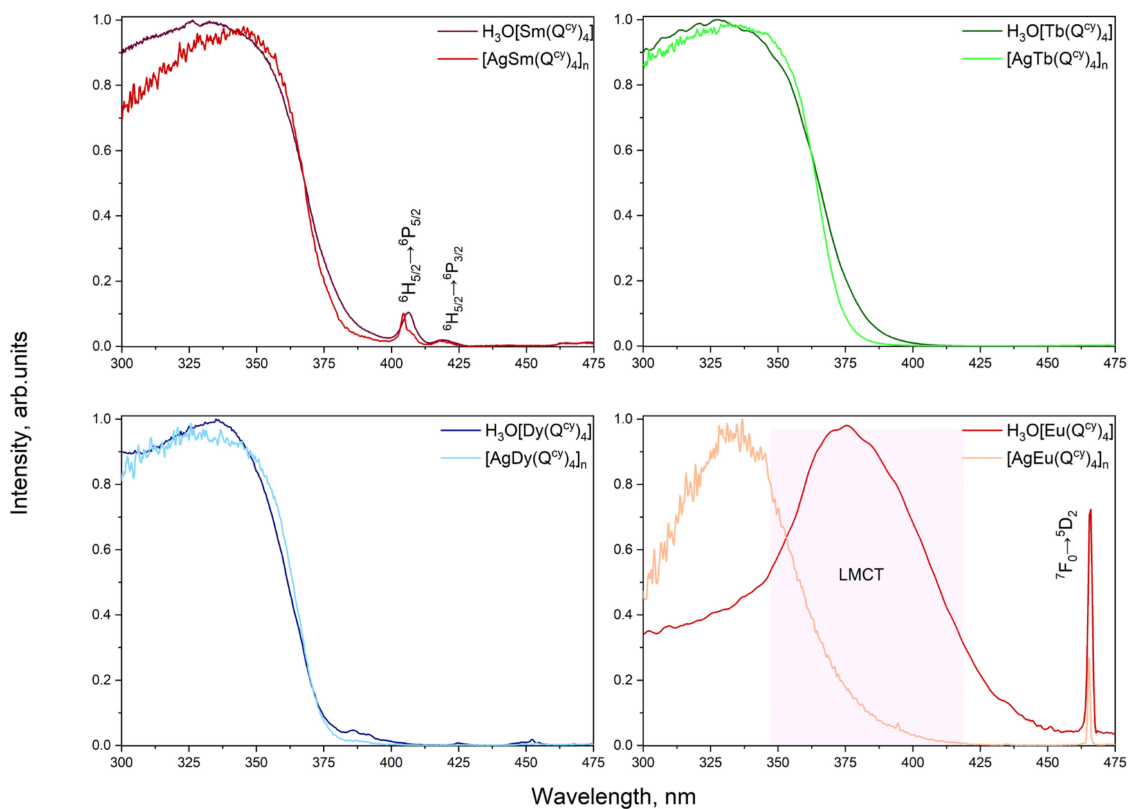

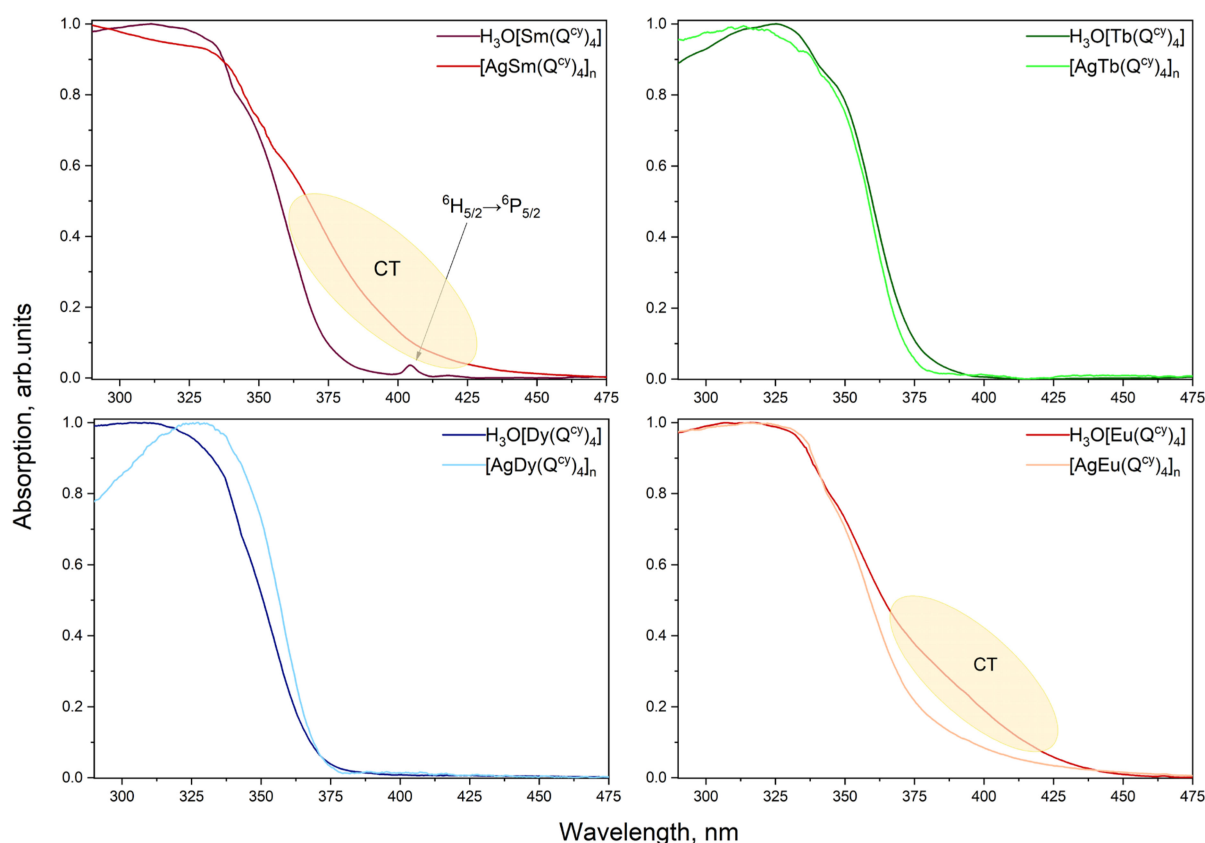**Figure 5.** PL excitation spectra for all the complexes pairwise.

Figure 6. Diffuse reflection spectra for all the complexes pairwise.

Interestingly, the spectra of complexes containing Ag$^+$ are qualitatively similar, while the diffuse reflection spectra (see Figure 6) of [AgSm(Q^{cy})$_4$]$_n$ **6** and [AgEu(Q^{cy})$_4$]$_n$ **7** also reveal charge transfer processes.

The weak narrow bands observed in the excitation spectra of **1** and **2** and of **6** and **7** are related to the $^4H_{5/2} \rightarrow {}^6P_{5/2}$ and $^4H_{5/2} \rightarrow {}^6P_{3/2}$ transitions of the Sm^{3+} ion and the $^7F_0 \rightarrow {}^5D_2$ transition of the Eu^{3+} ion. Such behavior implicitly proves effective energy transfer of electronic excitation from donor-ligand to acceptors-ions.

Intensive luminescence of all the investigated complexes is observed under optical excitation via absorption bands associated with ligand environment (see Figures 7–9). In all the ionic species, we observed the narrow spectral bands typical of *f**-*f* transitions (see Table S5). The correlation of the emission bands with the *f**-*f* transitions was performed according to [57,87,88]. Notably, we observed no ligand emission in the emission spectra, which also indicates the relatively effective energy transfer of electronic excitation from ligand to ions [26].

The luminescence spectra of the complexes containing H$_3$O$^+$ and Ag$^+$ have no significant differences pairwise in Stark splitting and emission band positions. Thereby, the replacement of H$_3$O$^+$ with the Ag$^+$ produces no change in the symmetry of coordination polyhedral [26,89,90].

PL decays were recorded under the excitation wavelengths corresponding to maxima of excitation spectra with the registration at the photoluminescence maxima (see Figures S3 and S4). However, all the decay curves were estimated by a biexponential function. The obtained characteristic lifetimes are presented in Table 3. The replacement of H$_3$O$^+$ with Ag$^+$ in the ligand environment leads to an increase of observed lifetimes for all the complexes except for Tb^{3+} ion complexes. Photoluminescence overall quantum yield (PLQY, ϕ) values recorded under UV excitation are presented in Table 3.

Table 3. PL quantum yields and PL decays characteristic lifetimes for Sm, Tb, Dy and Eu complexes.

Complex	λ_{exc}, nm	PLQY, %	λ_{reg}, nm	τ_1, µs	τ_2, µs
1	350	2.0	650	44.1 ± 0.5	73.6 ± 1.2
6	350	0.8	650	66.7 ± 3.1	88.2 ± 7.6
4	350	55.6	550	593.9 ± 4.8	1403.9 ± 1.9
9	350	14.8	550	292.9 ± 2.9	805.7 ± 1.6
5	350	2.8 [57]	570	13.0 ± 0.1	42.7 ± 0.1
10	350	1.0	570	25.3 ± 1.3	49.8 ± 0.1
2	370	n.a.	615	97.9 ± 0.5	486.9 ± 2.0
7	350	0.3	615	179.8 ± 2.2	592.5 ± 1.4
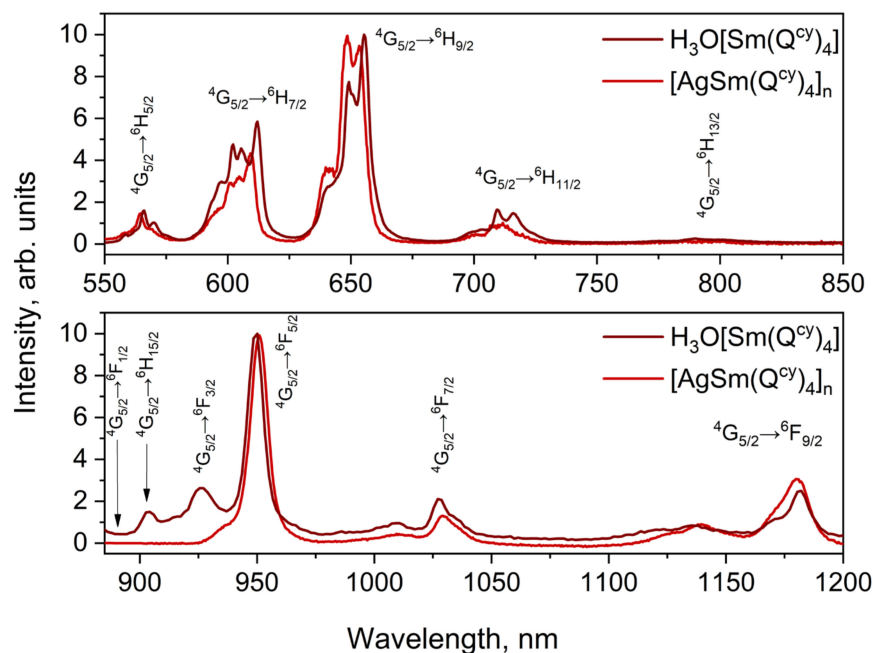
Figure 7. Photoluminescence spectra of Sm^{3+} complexes **1** and **6**.
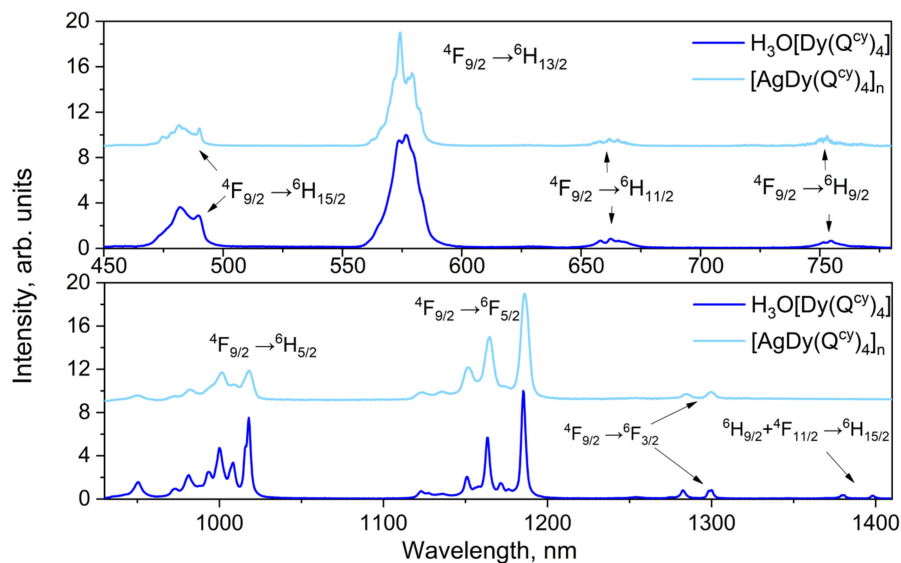
Figure 8. Photoluminescence spectra for Dy^{3+} complexes **5** and **10**.
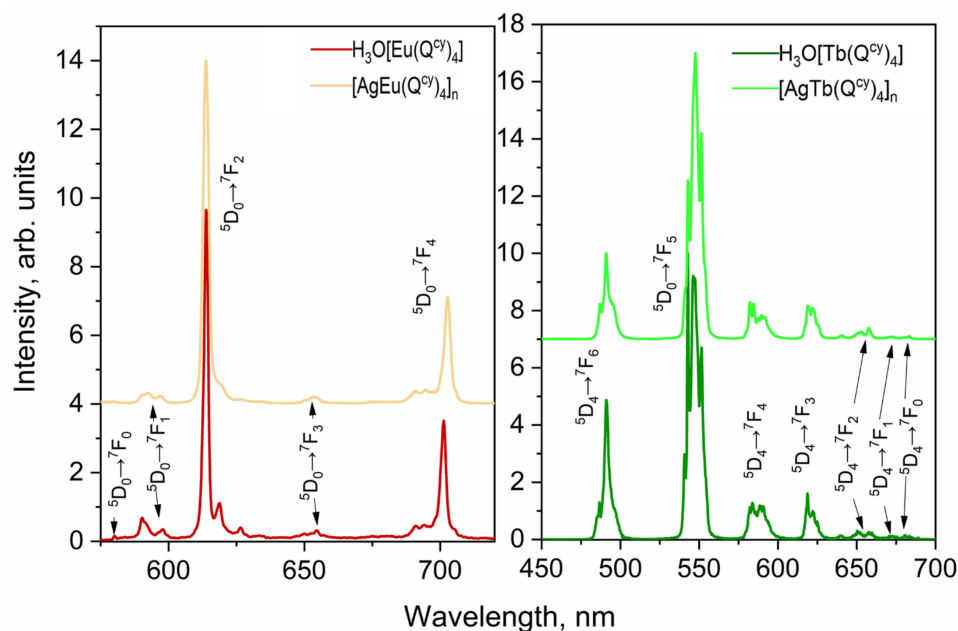
Figure 9. Photoluminescence spectra for Eu^{3+} (**2** and **7**) and Tb^{3+} (**4** and **9**) complexes.

To determine the triplet level energy of the ligand in lanthanide complexes, measurements of the low-temperature phosphorescence spectra of Gd^{3+} derivatives are usually used [26,91]. The combination of the high energy of the natural resonance level ($>30,000$ cm^{-1}) of Gd^{3+} ions, the paramagnetic nature and the heavy atom effect contribute to the fact that the low-temperature emission spectra of gadolinium complexes mainly contain a phosphorescence transition whose energy corresponds to the triplet level value [92].

The phosphorescence spectra measured at 77 K for the solid state Gd^{3+} complexes are shown in Figure S5. The energy of the first excited triplet state was derived from the maximum of the fitting component corresponding to the zero-phonon line in the spectrum, according to the well-known procedure [93]. Thus, based on the spectral and kinetic measurements, we were able to construct the Jablonsky–Crossby energy diagrams for complexes reported here (Figures 10 and 11). The luminescence characteristics of the europium complexes are caused by the influence of the LMCT state, which quenches the luminescence in the $H_3O[Eu(Q^{cy})_4]$ complex and is associated with the ease ($E^0_{Eu^{3+}/Eu^{2+}} = -0.35$ V) [86] reduction of the europium ion. The high oxidation potential ($E^0_{Ag^+/Ag} = 0.799$ V) of silver blocks this mechanism, which makes it possible to improve the luminescence characteristics of europium complexes. We believe that the low luminescence efficiency of other previously described europium acylpyrazolonates can also be explained by LMCT quenching [37,65].

The replacement of H_3O^+ with Ag^+ in the ligand environment results in a significant decrease of PLQY, except for the Eu^{3+} complexes. The distance between the ions in the crystal package decreases practically two times after the replacement of H_3O^+ with Ag^+, which results in cross-relaxation processes between the ions, which suppresses the radiative relaxation. Surprisingly, the Eu^{3+} complexes have low values of quantum yield; in particular, the ϕ of $[AgEu(Q^{cy})_4]_n$ is 0.3% and $H_3O[Eu(Q^{cy})_4]$ PLQY is lower than 0.005%.

All the complexes have rather low extinction coefficients for the absorption bands characteristic of the lanthanide ions (see Figure S6). However, we successfully performed the Judd-Ofelt analysis [94,95] for the $H_3O[Sm(Q^{cy})_4]$ complex to estimate the τ_{rad} radiative lifetime value for the $^4G_{5/2}$ emission state of the Sm^{3+} ion. The general procedure was the same as reported in [87]. It should be noted that for minimizing the root-mean-square deviation (RMS) in our calculations we include only transitions within the energy range 8000–22,000 cm^{-1}; see Table 4. The oscillator strengths of the electric dipole transitions determined from the optical absorption spectrum and calculated ones, Ω_t (t = 2,4,6) Judd–Ofelt intensity parameters and radiative rate of the emission state of Sm^{3+} ion in our

complex $H_3O[Sm(Q^{cy})_4]$ **1** are presented in Table 4. The refractive index value 1.47 was used in our calculations according to [96]. Theoretical branching ratios for luminescent transitions are in good agreement with the experimental data and the low RMS value allow us to consider our results to be accurate; see Table 5.
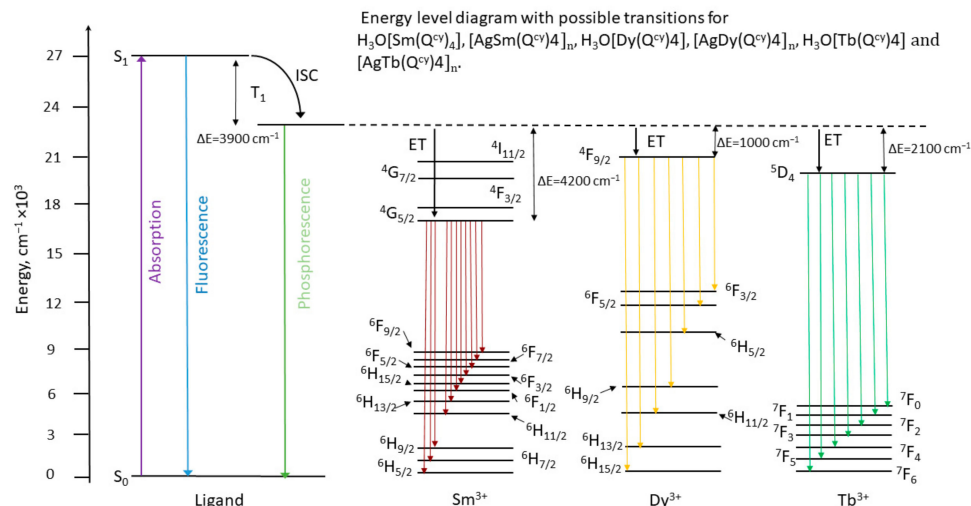

Figure 10. Energy diagram with possible transitions for **1** and **6** (Sm^{3+}), **5** and **10** (Dy^{3+}), **4** and **9** (Tb^{3+}).
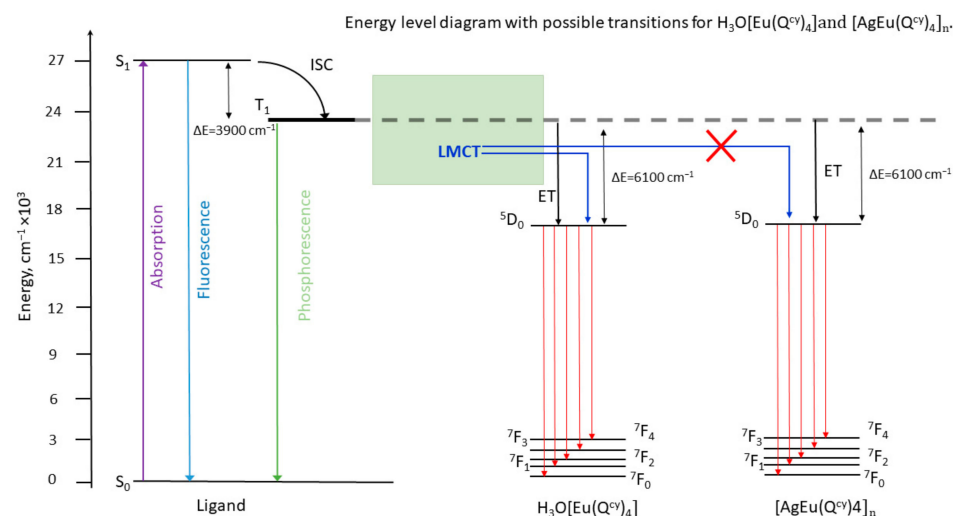

Figure 11. Energy diagram with possible transitions for $[H_3O][Eu(Q^{cy})_4]$ **2** and $[AgEu(Q^{cy})_4]_n$ **7**.

Table 4. Experimental f_{exp} and calculated f_{calc} oscillator strengths, Judd–Ofelt parameters Ω_t (t = 2,4,6), and root-mean-squared deviation RMS for complex $H_3O[Sm(Q^{cy})_4]$ **1**.

$^6H_{5/2} \rightarrow {}^{2S+1}L_J$	Wavelength, nm	$f_{exp} \times 10^8$	$f_{calc} \times 10^8$
$^6F_{7/2}$	1237	99.4	99.4
$^6F_{9/2}$	1086	49.0	49.2
$^6F_{11/2}$	948	8.5	7.4
$^4F_{5/2}$	454	1.6	1.8
Ω_2, cm^2			8.1×10^{-20}
Ω_4, cm^2			1.8×10^{-20}
Ω_6, cm^2			0.5×10^{-20}
	RMS $= 1.3 \times 10^{-8}$		

Table 5. Calculated electric-dipole transition probabilities A_{rad}, branching ratios β_{calc}, radiative lifetime τ_{rad} for complex $H_3O[Sm(Q^{cy})_4]$.

$^4G_{5/2} \rightarrow {}^{2S+1}L_J$	Wavelength, nm	A_{rad}, s^{-1}	β_{calc}, %
$^6H_{5/2}$	565	8.65	2.7
$^6H_{7/2}$	610	46.21	14.9
$^6H_{9/2}$	650	178.67	57.6
$^6H_{11/2}$	715	14.27	4.6
$^6H_{13/2}$	800	0.85	0.27
$^6F_{3/2}$	936	6.14	1.98
$^6F_{5/2}$	949	34.99	11.2
$^6F_{7/2}$	1036	1.47	0.47
$^6F_{9/2}$	1180	18.67	6.02
τ_{rad} = 3.2 ms; RMS = 1.3 × 10^{-8}			

The evaluated τ_{rad} value of ca. 3.2 ms is of the same order of magnitude of those reported for other Sm^{3+} complexes with similar chemical environments [87,97]. Measured luminescence decay times, obtained for the resonant excitation of the Sm^{3+} ion in the complex at 405 nm, are slightly higher than those presented in Table 5, and could also be fitted by a biexponential function with τ_1 = 49.1 ± 0.8 μs and τ_2 = 80.1 ± 1.4 μs. The estimated internal quantum yield of the complex is near 2% (1.5–2.4%, with respect to the biexponential luminescence decay behavior and accuracy of the calculations); the estimated and measured values are very close, and the sensibilization coefficient is close to 1.

The complexes reported in this work brightly emit in red, yellow and green spectral regions. For each compound, color diagrams were made (see Figure 12). The color coordinates for all the complexes are presented in Table S6.
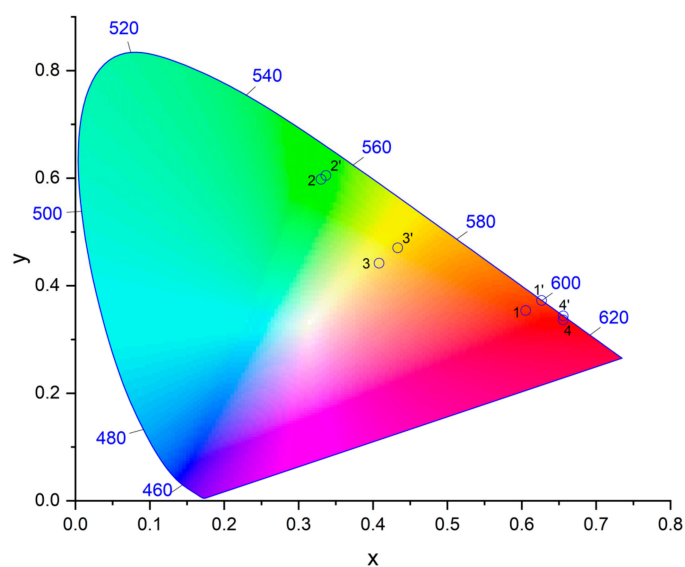
Figure 12. CIE diagram for complexes **1, 6, 2, 7, 3, 8, 4** and **9**.

The internal quantum yield can be estimated by the following formula

$$PLQY_{in} = \frac{k_{rad}}{k_{rad} + k_{nrad}}.$$

Since the rate constant of the magnetic-dipole transition $^5D_0 \rightarrow {}^7F_1$ in Eu^{3+}, $k_{MD}= 14.65$ s^{-1}, does not depend on the electric field induced by the ligand, the value of k_{rad} can be determined by the relationship:

$$k_{rad} = k_{MD} n^3 \frac{I_{tot}}{I_{MD}},$$

where n is the refractive index and $\frac{I_{tot}}{I_{MD}}$ is the ratio between the total integral luminescence intensity and the integral intensity of the magnetic-dipole transition. The k_{nrad} constant was estimated using a simple dependence:

$$k_{nrad} = \frac{1}{\tau_{obs}} - k_{rad}$$

comprising the calculated k_{rad} and the observed attenuation time τ_{obs} measured with resonant excitation of Eu^{3+} at a wavelength of 464 nm. The calculated internal quantum yields $PLQY_{in}$, the total quantum yields $PLQY$ measured by the absolute method, and the sensitization coefficients η are presented in Table 6.

Table 6. Photophysical parameters for complexes **2** and **7** in the solid state. Internal quantum yields Φ_{in} and sensitization coefficients η.

Complex	n	I_{tot}/I_{MD}	k_{rad}, s^{-1}	k_{nrad}, s^{-1}	$\tau_{obs}{}^{-1}$, s^{-1}	$PLQY_{in}$, %	PLQY, %	η
2		8.87	438	2000	2439	17.90	—	—
7	1.5	19.03	941	748	1689	55.70	0.3	0.05385

4. Conclusions

The synthesis of coordination polymers based on lanthanides acylpyrazolonates due to the formation of a heterometallic *4d-4f* complexes is shown for the first time. The resulting coordination polymers exhibit bright luminescence caused by *f-f* transitions of the central ions. The change from a monomeric to a polymeric structure leads to various changes in the luminescence characteristics: while for samarium, terbium, and dysprosium derivatives the luminescence efficiency somewhat decreases, in the case of europium, on the contrary, it increases significantly. This phenomenon is due to the special role of LMCT states in europium acylpyrazolonates.

Author Contributions: Conceptualization, Y.A.B., M.T.M. and C.P.; Data curation, M.T.M., D.A.M., M.A.K., I.A.Y. and T.A.P.; formal analysis, Y.A.B., M.T.M., M.A.K., D.A.M., C.P., A.A.D., I.V.T. and F.M.; funding acquisition, I.V.T. and C.P.; resources, I.V.T., Y.A.B., C.P. and A.A.D.; investigation, Y.A.B., M.T.M., D.A.M., T.A.P., M.A.K., I.A.Y. and I.V.T.; data curation, M.T.M., D.A.M., T.A.P., M.A.K. and I.A.Y.; writing—original draft preparation, Y.A.B., M.T.M., D.A.M. and A.A.D.; writing—review and editing, I.V.T., C.P. and F.M.; visualization, M.T.M., D.A.M., T.A.P. and M.A.K.; supervision, Y.A.B., A.A.D. and C.P.; project administration, I.V.T., C.P., F.M. and Y.A.B. All authors have read and agreed to the published version of the manuscript.

References

1. Cui, Y.; Yue, Y.; Qian, G.; Chen, B. Luminescent Functional Metal–Organic Frameworks. *Chem. Rev.* **2012**, *112*, 1126–1162. [CrossRef] [PubMed]
2. Lustig, W.P.; Li, J. Luminescent Metal–Organic Frameworks and Coordination Polymers as Alternative Phosphors for Energy Efficient Lighting Devices. *Coord. Chem. Rev.* **2018**, *373*, 116–147. [CrossRef]
3. Hasegawa, Y.; Nakanishi, T. Luminescent Lanthanide Coordination Polymers for Photonic Applications. *RSC Adv.* **2015**, *5*, 338–353. [CrossRef]
4. Li, B.; Wen, H.-M.; Cui, Y.; Qian, G.; Chen, B. Multifunctional Lanthanide Coordination Polymers. *Prog. Polym. Sci.* **2015**, *48*, 40–84. [CrossRef]
5. Belousov, Y.A.; Drozdov, A.A.; Taydakov, I.V.; Marchetti, F.; Pettinari, R.; Pettinari, C. Lanthanide Azolecarboxylate Compounds: Structure, Luminescent Properties and Applications. *Coord. Chem. Rev.* **2021**, *445*, 214084. [CrossRef]
6. Bünzli, J.C.G.; Piguet, C. Lanthanide-Containing Molecular and Supramolecular Polymetallic Functional Assemblies. *Chem. Rev.* **2002**, *102*, 1897–1928. [CrossRef]
7. Cotton, S. *Lanthanide and Actinide Chemistry*; John Wiley & Sons, Ltd: Chichester, UK, 2006; ISBN 9780470010082.
8. Xu, H.; Sun, Q.; An, Z.; Wei, Y.; Liu, X. Electroluminescence from Europium(III) Complexes. *Coord. Chem. Rev.* **2015**, *293–294*, 228–249. [CrossRef]
9. Álvarez, Á.L.; Coya, C. OLEDs Based on Ln(III) Complexes for near-Infrared Emission. In *Lanthanide-Based Multifunctional Materials*; Elsevier: Amsterdam, The Netherlands, 2018; pp. 133–170. ISBN 9780128138403.
10. Wang, L.; Zhao, Z.; Wei, C.; Wei, H.; Liu, Z.; Bian, Z.; Huang, C. Review on the Electroluminescence Study of Lanthanide Complexes. *Adv. Opt. Mater.* **2019**, *7*, 1801256. [CrossRef]
11. Zinna, F.; Pasini, M.; Galeotti, F.; Botta, C.; Di Bari, L.; Giovanella, U. Design of Lanthanide-Based OLEDs with Remarkable Circularly Polarized Electroluminescence. *Adv. Funct. Mater.* **2017**, *27*, 1603719. [CrossRef]
12. Dreyer, D.R.; Park, S.; Bielawski, C.W.; Ruoff, R.S. Lanthanide Luminescence for Functional Materials and Bio-Sciences. *Chem. Soc. Rev.* **2010**, *1*, 189–227. [CrossRef]
13. Heffern, M.C.; Matosziuk, L.M.; Meade, T.J. Lanthanide Probes for Bioresponsive Imaging. *Chem. Rev.* **2014**, *114*, 4496–4539. [CrossRef]
14. Yang, Y.; Zhao, Q.; Feng, W.; Li, F. Luminescent Chemodosimeters for Bioimaging. *Chem. Rev.* **2013**, *113*, 192–270. [CrossRef]
15. Grebenyuk, D.; Zobel, M.; Tsymbarenko, D. Partially Ordered Lanthanide Carboxylates with a Highly Adaptable 1D Polymeric Structure. *Polymers* **2022**, *14*, 3328. [CrossRef]
16. Brites, C.D.S.; Millán, A.; Carlos, L.D. Lanthanides in Luminescent Thermometry. In *Handbook on the Physics and Chemistry of Rare Earths*; Elsevier B.V.: Amsterdam, The Netherlands, 2016; Volume 49, pp. 339–427.
17. Rocha, J.; Brites, C.D.S.; Carlos, L.D. Lanthanide Organic Framework Luminescent Thermometers. *Chem. A Eur. J.* **2016**, *22*, 14782–14795. [CrossRef]
18. Lee, S.; Lin, M.; Lee, A.; Park, Y. Lanthanide-Doped Nanoparticles for Diagnostic Sensing. *Nanomaterials* **2017**, *7*, 411. [CrossRef]
19. Aulsebrook, M.L.; Graham, B.; Grace, M.R.; Tuck, K.L. Lanthanide Complexes for Luminescence-Based Sensing of Low Molecular Weight Analytes. *Coord. Chem. Rev.* **2018**, *375*, 191–220. [CrossRef]
20. Aletti, A.B.; Gillen, D.M.; Gunnlaugsson, T. Luminescent/Colorimetric Probes and (Chemo-) Sensors for Detecting Anions Based on Transition and Lanthanide Ion Receptor/Binding Complexes. *Coord. Chem. Rev.* **2018**, *354*, 98–120. [CrossRef]
21. Xu, H.; Cao, C.S.; Kang, X.M.; Zhao, B. Lanthanide-Based Metal-Organic Frameworks as Luminescent Probes. *Dalt. Trans.* **2016**, *45*, 18003–18017. [CrossRef]
22. Zhao, S.-N.; Wang, G.; Poelman, D.; Voort, P. Luminescent Lanthanide MOFs: A Unique Platform for Chemical Sensing. *Materials* **2018**, *11*, 572. [CrossRef]
23. Lunev, A.M.; Belousov, Y.A. Luminescent Sensor Materials Based on Rare-Earth Element Complexes for Detecting Cations, Anions, and Small Molecules. *Russ. Chem. Bull.* **2022**, *71*, 825–857. [CrossRef]
24. Crosby, G.A.; Whan, R.E.; Freeman, J.J. Spectroscopic Studies of Rare Earth Chelates. *J. Phys. Chem.* **1962**, *66*, 2493–2499. [CrossRef]
25. Bünzli, J.-C.G.; Piguet, C. Taking Advantage of Luminescent Lanthanide Ions. *Chem. Soc. Rev.* **2005**, *34*, 1048. [CrossRef]

26. Bünzli, J.; Eliseeva, S.V. Basics of Lanthanides Photophysics. In *Lanthanide Luminescence*; Hänninen, P., Härmä, H., Eds.; Springer Series on Fluorescence; Springer: Berlin/Heidelberg, Germany, 2010; Volume 7, pp. 1–45. [CrossRef]

27. Nehra, K.; Dalal, A.; Hooda, A.; Bhagwan, S.; Saini, R.K.; Mari, B.; Kumar, S.; Singh, D. Lanthanides β-Diketonate Complexes as Energy-Efficient Emissive Materials: A Review. *J. Mol. Struct.* **2022**, *1249*, 131531. [CrossRef]

28. Janicki, R.; Mondry, A.; Starynowicz, P. Carboxylates of Rare Earth Elements. *Coord. Chem. Rev.* **2017**, *340*, 98–133. [CrossRef]

29. Taidakov, I.V.; Lobanov, A.N.; Vitukhnovskii, A.G.; Starikova, Z.A. Synthesis and Unusual Crystal Structure of the Eu(III) Complex with 1-(1,5-Dimethyl-1H-Pyrazol-4-Yl)-4,4,4-Trifluorobutane-1,3-Dione. *Russ. J. Coord. Chem.* **2013**, *39*, 437–441. [CrossRef]

30. Yang, P. Synthesis, Structure, and Luminescence Properties of Rare Earth Complexes with β-Diketone Containing Imidazole Group. *Z. Anorg. Allg. Chem.* **2018**, *644*, 838–843. [CrossRef]

31. Burrows, A.D.; Mahon, M.F.; Renouf, C.L.; Richardson, C.; Warren, A.J.; Warren, J.E. Dipyridyl β-Diketonate Complexes and Their Use as Metalloligands in the Formation of Mixed-Metal Coordination Networks. *Dalt. Trans.* **2012**, *41*, 4153. [CrossRef]

32. Hui, Y.-C.; Meng, Y.-S.; Li, Z.; Chen, Q.; Sun, H.-L.; Zhang, Y.-Q.; Gao, S. Construction and Theoretical Study of a New Dy-β-Diketone Chain Featuring Slow Magnetic Relaxation. *CrystEngComm* **2015**, *17*, 5620–5624. [CrossRef]

33. Liu, F.; Zhou, Y. Polymeric [Eu(L)₃(H₂O)] (HL = 1-(Pyridin-4-Yl)Butane- 1,3-Dione and Dimeric [Eu₂(L)₆(H₂O)₂] (HL = 1,3-Di(Pyridin-3-Yl)Propane-1,3-Dione) as Selective and Sensitive Chemosensors for Hg(II) Ion. *Inorg. Chem. Commun.* **2010**, *13*, 1410–1413. [CrossRef]

34. Guettas, D.; Montigaud, V.; Garcia, G.F.; Larini, P.; Cador, O.; Le Guennic, B.; Pilet, G. Fine Control of the Metal Environment within Dysprosium-Based Mononuclear Single-Molecule Magnets. *Eur. J. Inorg. Chem.* **2018**, *2018*, 333–339. [CrossRef]

35. Andrews, P.C.; Deacon, G.B.; Frank, R.; Fraser, B.H.; Junk, P.C.; MacLellan, J.G.; Massi, M.; Moubaraki, B.; Murray, K.S.; Silberstein, M. Formation of Ho III Trinuclear Clusters and Gd III Monodimensional Polymers Induced by Ortho and Para Regioisomers of Pyridyl-Functionalised B-Diketones: Synthesis, Structure, and Magnetic Properties. *Eur. J. Inorg. Chem.* **2009**, *2009*, 744–751. [CrossRef]

36. Semenov, S.N.; Rogachev, A.Y.; Eliseeva, S.V.; Pettinari, C.; Marchetti, F.; Drozdov, A.A.; Troyanov, S.I. First Direct Assembly of Molecular Helical Complexes into a Coordination Polymer. *Chem. Commun.* **2008**, *17*, 1992–1994. [CrossRef]

37. Marchetti, F.; Pettinari, C.; Pizzabiocca, A.; Drozdov, A.A.; Troyanov, S.I.; Zhuravlev, C.O.; Semenov, S.N.; Belousov, Y.A.; Timokhin, I.G. Syntheses, Structures, and Spectroscopy of Mono- and Polynuclear Lanthanide Complexes Containing 4-Acyl-Pyrazolones and Diphosphineoxide. *Inorg. Chim. Acta* **2010**, *363*, 4038–4047. [CrossRef]

38. Miyata, K.; Ohba, T.; Kobayashi, A.; Kato, M.; Nakanishi, T.; Fushimi, K.; Hasegawa, Y. Thermostable Organo-Phosphor: Low-Vibrational Coordination Polymers That Exhibit Different Intermolecular Interactions. *Chempluschem* **2012**, *77*, 277–280. [CrossRef]

39. Hasegawa, Y.; Miura, Y.; Kitagawa, Y.; Wada, S.; Nakanishi, T.; Fushimi, K.; Seki, T.; Ito, H.; Iwasa, T.; Taketsugu, T.; et al. Spiral Eu(iii) Coordination Polymers with Circularly Polarized Luminescence. *Chem. Commun.* **2018**, *54*, 10695–10697. [CrossRef]

40. Kitagawa, Y.; Naito, A.; Fushimi, K.; Hasegawa, Y. Bright Sky-Blue Fluorescence with High Color Purity: Assembly of Luminescent Diphenyl-Anthracene Lutetium-Based Coordination Polymer. *RSC Adv.* **2021**, *11*, 6604–6606. [CrossRef]

41. Zhang, L.; Chen, P.; Li, H.-F.; Tian, Y.-M.; Yan, P.-F.; Sun, W.-B. From Zero-Dimensional to One-Dimensional Chain N -Oxide Bridged Compounds with Enhanced Single-Molecule Magnetic Performance. *Dalt. Trans.* **2019**, *48*, 4324–4332. [CrossRef]

42. Hirai, Y.; Ferreira Da Rosa, P.P.; Nakanishi, T.; Kitagawa, Y.; Fushimi, K.; Seki, T.; Ito, H.; Hasegawa, Y. Structural Manipulation of Triboluminescent Lanthanide Coordination Polymers by Side-Group Alteration. *Inorg. Chem.* **2018**, *57*, 14653–14659. [CrossRef]

43. Armelao, L.; Belli Dell'Amico, D.; Bellucci, L.; Bottaro, G.; Labella, L.; Marchetti, F.; Samaritani, S. A Convenient Synthesis of Highly Luminescent Lanthanide 1D-Zigzag Coordination Chains Based Only on 4,4′-Bipyridine as Connector. *Polyhedron* **2016**, *119*, 371–376. [CrossRef]

44. Wang, J.; Yang, M.; Sun, J.; Li, H.; Liu, J.; Wang, Q.; Li, L.; Ma, Y.; Zhao, B.; Cheng, P. Enhancing the Energy Barrier of Dysprosium(iii) Single-Molecule Magnets by Tuning the Magnetic Interactions through Different N -Oxide Bridging Ligands. *CrystEngComm* **2019**, *21*, 6219–6225. [CrossRef]

45. Flores Gonzalez, J.; Cador, O.; Ouahab, L.; Norkov, S.; Kuropatov, V.; Pointillart, F. Field-Induced Dysprosium Single-Molecule Magnet Involving a Fused o-Semiquinone-Extended-Tetrathiafulvalene-o-Semiquinone Bridging Triad. *Inorganics* **2018**, *6*, 45. [CrossRef]

46. Fratini, A.; Richards, G.; Larder, E.; Swavey, S. Neodymium, Gadolinium, and Terbium Complexes Containing Hexafluoroacetylacetonate and 2,2′-Bipyrimidine: Structural and Spectroscopic Characterization. *Inorg. Chem.* **2008**, *47*, 1030–1036. [CrossRef] [PubMed]

47. Tan, R.H.C.; Motevalli, M.; Abrahams, I.; Wyatt, P.B.; Gillin, W.P. Quenching of IR Luminescence of Erbium, Neodymium, and Ytterbium β-Diketonate Complexes by Ligand C−H and C−D Bonds. *J. Phys. Chem. B* **2006**, *110*, 24476–24479. [CrossRef] [PubMed]

48. Mara, D.; Artizzu, F.; Laforce, B.; Vincze, L.; Van Hecke, K.; Van Deun, R.; Kaczmarek, A.M. Novel Tetrakis Lanthanide β-Diketonate Complexes: Structural Study, Luminescence Properties and Temperature Sensing. *J. Lumin.* **2019**, *213*, 343–355. [CrossRef]

49. Abad Galán, L.; Sobolev, A.N.; Zysman-Colman, E.; Ogden, M.I.; Massi, M. Lanthanoid Complexes Supported by Retro-Claisen Condensation Products of β-Triketonates. *Dalt. Trans.* **2018**, *47*, 17469–17478. [CrossRef]

50. Marchetti, F.; Pettinari, C.; Pettinari, R. Acylpyrazolone Ligands: Synthesis, Structures, Metal Coordination Chemistry and Applications. *Coord. Chem. Rev.* **2005**, *249*, 2909–2945. [CrossRef]

51. Marchetti, F.; Pettinari, R.; Pettinari, C. Recent Advances in Acylpyrazolone Metal Complexes and Their Potential Applications. *Coord. Chem. Rev.* **2015**, *303*, 1–31. [CrossRef]

52. Belousov, Y.A.; Drozdov, A.A. Lanthanide Acylpyrazolonates: Synthesis, Properties and Structural Features. *Russ. Chem. Rev.* **2012**, *81*, 1159–1169. [CrossRef]

53. Capecchi, S.; Renault, O.; Moon, D.G.; Halim, M.; Etchells, M.; Dobson, P.J.; Salata, O.V.; Christou, V. High-Efficiency Organic Electroluminescent Devices Using an Organoterbium Emitter. *Adv. Mater.* **2000**, *12*, 1591–1594. [CrossRef]

54. Thorne, J.R.G.; Rey, J.M.; Denning, R.G.; Watkins, S.E.; Etchells, M.; Green, M.; Christou, V. Excited State Dynamics of Organo-Lanthanide Electroluminescent Phosphors: The Properties of Tb(Tb-Pmp)3 and Gd(Tb-Pmp)3. *J. Phys. Chem. A* **2002**, *106*, 4014–4021. [CrossRef]

55. Chen, Z.; Ding, F.; Hao, F.; Bian, Z.; Ding, B.; Zhu, Y.; Chen, F.; Huang, C. A Highly Efficient OLED Based on Terbium Complexes. *Org. Electron.* **2009**, *10*, 939–947. [CrossRef]

56. Girotto, E.; Pereira, A.; Arantes, C.; Cremona, M.; Bortoluzzi, A.J.; Salla, C.A.M.; Bechtold, I.H.; Gallardo, H. Efficient Terbium Complex Based on a Novel Pyrazolone Derivative Ligand Used in Solution-Processed OLEDs. *J. Lumin.* **2019**, *208*, 57–62. [CrossRef]

57. Belousov, Y.A.; Korshunov, V.M.; Metlin, M.T.; Metlina, D.A.; Kiskin, M.A.; Aminev, D.F.; Datskevich, N.P.; Drozdov, A.A.; Pettinari, C.; Marchetti, F.; et al. Towards Bright Dysprosium Emitters: Single and Combined Effects of Environmental Symmetry, Deuteration, and Gadolinium Dilution. *Dye. Pigment.* **2022**, *199*, 110078. [CrossRef]

58. Li, Z.F.; Zhou, L.; Yu, J.B.; Zhang, H.J.; Deng, R.P.; Peng, Z.P.; Guo, Z.Y. Synthesis, Structure, Photoluminescence, and Electroluminescence Properties of a New Dysprosium Complex. *J. Phys. Chem. C* **2007**, *111*, 2295–2300. [CrossRef]

59. Li, X.L.; Li, J.; Zhu, C.; Han, B.; Liu, Y.; Yin, Z.; Li, F.; Liu, C.M. An Intense Luminescent Dy(iii) Single-Ion Magnet with the Acylpyrazolonate Ligand Showing Two Slow Magnetic Relaxation Processes. *New J. Chem.* **2018**, *42*, 16992–16998. [CrossRef]

60. Pettinari, C.; Marchetti, F.; Pettinari, R.; Drozdov, A.; Troyanov, S.; Voloshin, A.I.; Shavaleev, N.M. Synthesis, Structure and Luminescence Properties of New Rare Earth Metal Complexes with 1-Phenyl-3-Methyl-4-Acylpyrazol-5-Ones. *J. Chem. Soc. Dalt. Trans.* **2002**, *7*, 1409–1415. [CrossRef]

61. Zhang, D.; Shi, M.; Liu, Z.; Li, F.; Yi, T.; Huang, C. Luminescence Modulation of a Terbium Complex with Anions and Its Application as a Reagent. *Eur. J. Inorg. Chem.* **2006**, *3*, 2277–2284. [CrossRef]

62. Shen, L.; Shi, M.; Li, F.; Zhang, D.; Li, X.; Shi, E.; Yi, T.; Du, Y.; Huang, C. Polyaryl Ether Dendrimer with a 4-Phenylacetyl-5-Pyrazolone-Based Terbium(III) Complex as Core: Synthesis and Photopysical Properties. *Inorg. Chem.* **2006**, *45*, 6188–6197. [CrossRef]

63. Liu, J.; Shi, Q.; He, Y.; Fu, G.; Li, W.; Miao, T.; Lü, X. Single-Molecule White-Light of Tris-Pyrazolonate-Dy^{3+} Complexes. *Inorg. Chem. Commun.* **2019**, *109*, 107573. [CrossRef]

64. Xin, H.; Shi, M.; Zhang, X.M.; Li, F.Y.; Bian, Z.Q.; Ibrahim, K.; Liu, F.Q.; Huang, C.H. Carrier-Transport, Photoluminescence, and Electroluminescence Properties Comparison of a Series of Terbium Complexes with Different Structures. *Chem. Mater.* **2003**, *15*, 3728–3733. [CrossRef]

65. Taydakov, I.V.; Belousov, Y.A.; Lyssenko, K.A.; Varaksina, E.; Drozdov, A.A.; Marchetti, F.; Pettinari, R.; Pettinari, C. Synthesis, Phosphorescence and Luminescence Properties of Novel Europium and Gadolinium Tris-Acylpyrazolonate Complexes. *Inorg. Chim. Acta* **2020**, *502*, 119279. [CrossRef]

66. Li, J.; Zhang, L.; Liu, L.; Liu, G.; Jia, D.; Xu, G. A Series of Pyrazolone Lanthanide (III) Complexes: Synthesis, Crystal Structures and Fluorescence. *Inorg. Chim. Acta* **2007**, *360*, 1995–2001. [CrossRef]

67. Pettinari, C.; Marchetti, F.; Pettinari, R.; Drozdov, A.; Semenov, S.; Troyanov, S.I.; Zolin, V. A New Rare-Earth Metal Acylpyrazolonate Containing the Zundel Ion H$_5$O$_2^+$ Stabilized by Strong Hydrogen Bonding. *Inorg. Chem. Commun.* **2006**, *9*, 634–637. [CrossRef]

68. Pettinari, C.; Marchetti, F.; Pettinari, R.; Natanti, P.; Drozdov, A.; Semenov, S.; Troyanov, S.I.; Zolin, V. Syntheses, spectroscopic characterization and X-ray structural studies of lanthanide complexes with adamantyl substituted 4-acylpyrazol-5-one. *Inorg. Chim. Acta* **2006**, *359*, 4063–4070. [CrossRef]

69. Pettinari, C.; Marchetti, F.; Cingolani, A.; Drozdov, A.; Troyanov, S.; Timokhin, I.; Vertlib, V. Lanthanide Metal Complexes Containing the First Structurally Characterized β-Diketonate Acid Stabilized by Hydrogen Bonding. *Inorg. Chem. Commun.* **2003**, *6*, 48–51. [CrossRef]

70. Sukhikh, T.S.; Kolybalov, D.S.; Pylova, E.K.; Bashirov, D.A.; Komarov, V.Y.; Kuratieva, N.V.; Smolentsev, A.I.; Fitch, A.N.; Konchenko, S.N. A Fresh Look at the Structural Diversity of Dibenzoylmethanide Complexes of Lanthanides. *New J. Chem.* **2019**, *43*, 9934–9942. [CrossRef]

71. Safronova, A.V.; Bochkarev, L.N.; Baranov, E.V. Synthesis of Lanthanide Pyrazolonate Complexes by the Reactions of 1-Phenyl-3-Methyl-4-(2,2-Dimethylpropan-1-Oyl)Pyrazol-5-One with Metallic Lanthanides. Crystal Structures of [Ln(Bu t -PMP)3] 2 (Ln = Gd, Tb, and Tm). *Russ. J. Coord. Chem. Khimiya* **2013**, *39*, 537–543. [CrossRef]

72. Safronova, A.V.; Bochkarev, L.N.; Malysheva, I.P.; Baranov, E. V Inorganica Chimica Acta Facile Synthesis of Rare-Earth Pyrazolonates by the Reaction of Rare-Earth Metals with 1-Phenyl-3-Methyl-4-Isobutyryl-5-Pyrazolone. Crystal Structures of [Ln(PMIP)$_3$]$_2$ (Ln = Y, Gd, Tb, Er, Tm). *Inorg. Chim. Acta* **2012**, *392*, 454–458. [CrossRef]

73. Cingolani, A.; Effendy; Marchetti, F.; Pettinari, C.; Pettinari, R.; Skelton, B.W.; White, A.H. First Structurally Characterized Silver(I) Derivatives with Nonfluorinated β-Diketones. *Inorg. Chem.* **2002**, *41*, 1151–1161. [CrossRef]

74. Marchetti, F.; Palmucci, J.; Pettinari, C.; Pettinari, R.; Condello, F.; Ferraro, S.; Marangoni, M.; Crispini, A.; Scuri, S.; Grappasonni, I.; et al. Novel Composite Plastics Containing Silver(I) Acylpyrazolonato Additives Display Potent Antimicrobial Activity by Contact. *Chem. A Eur. J.* **2015**, *21*, 836–850. [CrossRef]

75. Bui, A.T.; Roux, A.; Grichine, A.; Duperray, A.; Andraud, C.; Maury, O. Twisted Charge-Transfer Antennae for Ultra-Bright Terbium(III) and Dysprosium(III) Bioprobes. *Chem. A Eur. J.* **2018**, *24*, 3408–3412. [CrossRef]

76. Lo, W.-S.; Zhang, J.; Wong, W.-T.; Law, G.-L. Highly Luminescent Sm III Complexes with Intraligand Charge-Transfer Sensitization and the Effect of Solvent Polarity on Their Luminescent Properties. *Inorg. Chem.* **2015**, *54*, 3725–3727. [CrossRef]

77. Barge, A.; Cravotto, G.; Gianolio, E.; Fedeli, F. How to Determine Free Gd and Free Ligand in Solution of Gd Chelates. A Technical Note. *Contrast Media Mol. Imaging* **2006**, *1*, 184–188. [CrossRef]

78. Hillebrand, W.F.; Lundell, G.E.F. *Applied Inorganic Analysis*; John Wiley & Sons, Ltd: New York City, NY, USA, 1929.

79. *SMART (Control) and SAINT (Integration) Software*, Version 5.0; Bruker AXS Inc.: Madison, WI, USA, 1997.

80. Svetogorov, R.D.; Dorovatovskii, P.V.; Lazarenko, V.A. Belok/XSA Diffraction Beamline for Studying Crystalline Samples at Kurchatov Synchrotron Radiation Source. *Cryst. Res. Technol.* **2020**, *55*, 1900184. [CrossRef]

81. Sheldrick, G.M. A Short History of SHELX. *Acta Crystallogr. Sect. A Found. Adv.* **2008**, *64*, 112–122. [CrossRef]

82. Dolomanov, O.V.; Bourhis, L.J.; Gildea, R.J.; Howard, J.A.K.; Puschmann, H. OLEX2: A Complete Structure Solution, Refinement and Analysis Program. *J. Appl. Crystallogr.* **2009**, *42*, 339–341. [CrossRef]

83. van der Sluis, P.; Spek, A.L. BYPASS: An Effective Method for the Refinement of Crystal Structures Containing Disordered Solvent Regions. *Acta Crystallogr. Sect. A Found. Crystallogr. Adv.* **1990**, *46*, 194–201. [CrossRef]

84. Kordeyro Magrino, D.A.; Korshunov, V.M.; Lyssenko, K.A.; Gontcharenko, V.E.; Belousov, Y.A.; Pettinari, C.; Taydakov, I. V Luminescent Complexes of Eu3+,Tb3+ and Gd3+ Nitrates with Polytopic Ligand 2,4,6-Tris(1H-Pyrazol-1-Yl)-1,3,5-Triazine. *Inorg. Chim. Acta* **2020**, *510*, 119764. [CrossRef]

85. Alexandrov, E.V.; Blatov, V.A.; Proserpio, D.M. How 2-Periodic Coordination Networks Are Interweaved: Entanglement Isomerism and Polymorphism. *CrystEngComm* **2017**, *19*, 1993–2006. [CrossRef]

86. Kovacs, D.; Borbas, K.E. The Role of Photoinduced Electron Transfer in the Quenching of Sensitized Europium Emission. *Coord. Chem. Rev.* **2018**, *364*, 1–9. [CrossRef]

87. Sizov, V.S.; Komissar, D.A.; Metlina, D.A.; Aminev, D.F.; Ambrozevich, S.A.; Nefedov, S.E.; Varaksina, E.A.; Metlin, M.T.; Mislavskií, V.V.; Taydakov, I.V. Effect of Ancillary Ligands on Visible and NIR Luminescence of Sm3+ β-Diketonate Complexes. *Spectrochim. Acta Part A Mol. Biomol. Spectrosc.* **2020**, *225*, 117503. [CrossRef] [PubMed]

88. Gontcharenko, V.E.; Kiskin, M.A.; Dolzhenko, V.D.; Korshunov, V.M.; Taydakov, I.V.; Belousov, Y.A. Mono- and Mixed Metal Complexes of Eu3+, Gd3+, and Tb3+ with a Diketone, Bearing Pyrazole Moiety and Chf2-Group: Structure, Color Tuning, and Kinetics of Energy Transfer between Lanthanide Ions. *Molecules* **2021**, *26*, 2655. [CrossRef] [PubMed]

89. Binnemans, K. Interpretation of Europium (III) Spectra. *Coord. Chem. Rev.* **2015**, *295*, 1–45. [CrossRef]

90. Vicentini, G.; Zinner, L.B.; Zukerman-Schpector, J.; Zinner, K. Luminescence and Structure of Europium Compounds. *Coord. Chem. Rev.* **2000**, *196*, 353–382. [CrossRef]

91. Sato, S.; Wada, M. Relations between Intramolecular Energy Transfer Efficiencies and Triplet State Energies in Rare Earth β-Diketone Chelates. *Bull. Chem. Soc. Jpn.* **1970**, *43*, 1955–1962. [CrossRef]

92. Latva, M.; Takalob, H.; Mukkala, V.M.; Matachescu, C.; Rodríguez-Ubis, J.C.; Kankare, J. Correlation between the Lowest Triplet State Energy Level of the Ligand and Lanthanide(III) Luminescence Quantum Yield. *J. Lumin.* **1997**, *75*, 149–169. [CrossRef]

93. Lewis, G.N.; Kasha, M. Phosphorescence and the Triplet State. *J. Am. Chem. Soc.* **1944**, *66*, 2100–2116. [CrossRef]

94. Judd, B.R. Optical Absorption Intensities of Rare-Earth Ions. *Phys. Rev.* **1962**, *127*, 750–761. [CrossRef]

95. Opelt, G.S. Intensities of Crystal Spectra of Rare-Earth Ions. *J. Chem. Phys.* **1962**, *37*, 511–520. [CrossRef]

96. Kozma, I.Z.; Krok, P.; Riedle, E. Direct Measurement of the Group-Velocity Mismatch and Derivation of the Refractive-Index Dispersion for a Variety of Solvents in the Ultraviolet. *J. Opt. Soc. Am. B* **2005**, *22*, 1479. [CrossRef]

97. Liang, H.; Xie, F. Optical Investigation of Sm(III)-β-Diketonate Complexes with Different Neutral Ligands. *Spectrochim. Acta Part A: Mol. Biomol. Spectrosc.* **2009**, *73*, 309–312. [CrossRef]

98. Casanova, D.; Llunell, M.; Alemany, P.; Alvarez, S. The Rich Stereochemistry of Eight-Vertex Polyhedra: A Continuous Shape Measures Study. *Chem. A Eur. J.* **2005**, *11*, 1479–1494. [CrossRef]